

Fabrication, temperature stability and characteristics of $\text{Pb}(\text{Zr}_x\text{Ti}_{1-x})\text{O}_3$ – $\text{Pb}(\text{Zn}_{1/3}\text{Nb}_{2/3})\text{O}_3$ – $\text{Pb}(\text{Ni}_{1/3}\text{Nb}_{2/3})\text{O}_3$ piezoelectric ceramics bimorph

Xiaolian Chao^{a,b}, Lili Yang^{a,b}, Hong Pan^{a,b}, Zupei Yang^{a,b,*}

^a Key Laboratory for Macromolecular Science of Shaanxi Province, Xi'an, 710062 Shaanxi, PR China

^b School of Chemistry and Materials Science, Shaanxi Normal University, Xi'an, 710062 Shaanxi, PR China

Received 26 October 2011; received in revised form 19 December 2011; accepted 19 December 2011

Available online 28 December 2011

Abstract

The phase structure, microstructure, electrical properties and the temperature stabilities of $\text{Pb}(\text{Zr}_x\text{Ti}_{1-x})\text{O}_3$ – $\text{Pb}(\text{Zn}_{1/3}\text{Nb}_{2/3})\text{O}_3$ – $\text{Pb}(\text{Ni}_{1/3}\text{Nb}_{2/3})\text{O}_3$ (PZT–PZN–PNN) ceramics are investigated in order to identify the morphotropic phase boundary composition in this system. The pure perovskite structure could be confirmed in all ceramics. The ceramics obtains the optimal piezoelectric properties at Zr/Ti ratio = 0.985, which are listed as follows: $d_{33} = 552$ pC/N, $K_p = 0.77$, $Q_m = 70$, $\tan \delta = 0.0150$ and $\epsilon_r = 2659$. When Zr/Ti ratio is 0.985, the values of $\Delta f_r/f_{r25^\circ\text{C}}$ and $\Delta K_p/K_{p25^\circ\text{C}}$ curves fluctuate around the zero, which indicate that the favorable temperature stability are obtained. Meanwhile, piezoelectric ceramics bimorph using PZT–PZN–PNN ceramics with Zr/Ti ratio of 0.985 is fabricated successfully by the tape-casting technology. The piezoelectric ceramics bimorph sintered at 1000 °C exhibits a larger displacement of 1683 μm at the working voltage of 180 V. The results indicate that the piezoelectric ceramics bimorph meets the needs of the needle selecting mechanism of electronic jacquard.

© 2012 Elsevier Ltd and Techna Group S.r.l. All rights reserved.

Keywords: C. Dielectric properties; C. Piezoelectric properties; Planar coupling coefficient; Piezoelectric ceramics bimorph

1. Introduction

Lead-based perovskite ferroelectric solid solution materials are of great interest for electromechanical transduction applications such as bimorphs, sensors, actuators chip-type piezoelectric actuators and ultrasonic motors [1,2]. Bimorphs have many advantages, which are micro-displacement, quick response, low driving voltage, low noise, etc. The ceramics suitable for the application of bimorphs should generate large displacement. It need the materials have high piezoelectric constant (d_{33}), high electromechanical coupling factor (k_p), low mechanical quality factor (Q_m), etc. [3].

In order to meet the above requirements, a number of piezoelectric ceramic systems have been developed, such as

$0.3\text{Pb}(\text{Zn}_{1/3}\text{Nb}_{2/3})\text{O}_3$ – $0.7\text{Pb}_{0.96}\text{La}_{0.04}(\text{Zr}_x\text{Ti}_{1-x})_{0.99}\text{O}_3$ [4], $\text{Pb}(\text{Mg}_{1/2}\text{W}_{1/2})\text{O}_3$ – $\text{Pb}(\text{Ni}_{1/3}\text{Nb}_{2/3})\text{O}_3$ – PbTiO_3 – PbZrO_3 [5] and $\text{Pb}(\text{Mg}_{1/3}\text{Nb}_{2/3})\text{O}_3$ – $\text{Pb}(\text{Zn}_{1/3}\text{Nb}_{2/3})\text{O}_3$ – $\text{Pb}(\text{Zr}_{0.52}\text{Ti}_{0.48})\text{O}_3$ [6]. However, high K_p , d_{33} , low Q_m and $\tan \delta$ of the above systems can be hardly simultaneously obtained at low sintering temperature. Moreover, the favorable temperature stabilities, the enhanced properties and low sintering temperatures of piezoelectric materials are important to the requirement of the piezoelectric ceramics bimorph. However, so far, there is still lack of study on the temperature stabilities and application of the piezoelectric ceramics bimorph [7–10].

The purpose of this paper is to investigate the phase structure, electrical properties and the temperature stability of PZT–PNN–PZN ceramics with different Zr/Ti ratios, and to provide promising candidates for piezoelectric ceramics bimorph applications. To satisfy the requirement of the needle selecting mechanism of electronic jacquard, the piezoelectric ceramics bimorph with the favorable composition are fabricated by the tape-casting method, which can provide a large workspace and high precision at the same time.

* Corresponding author at: Key Laboratory for Macromolecular Science of Shaanxi Province, School of Chemistry and Materials Science, Shaanxi Normal University, Xi'an, 710062 Shaanxi, PR China. Tel.: +86 29 8531 0352; fax: +86 29 8530 7774.

E-mail address: yangzp@snnu.edu.cn (Z. Yang).

2. Experimental procedure

The ceramics were synthesized by solid state reaction method. The compositions were as follows: $\text{Pb}(\text{Zr}_x\text{Ti}_{1-x})\text{O}_3\text{--Pb}(\text{Zn}_{1/3}\text{Nb}_{2/3})\text{O}_3\text{--Pb}(\text{Ni}_{1/3}\text{Nb}_{2/3})\text{O}_3$ ($x/y = 0.720, 0.777, 0.839, 0.905, 0.956, 0.985, 1.041$). The starting materials were Pb_3O_4 (97%), ZrO_2 (99%), TiO_2 (98%), Nb_2O_5 (99.5%), NiO (99%), ZnO (99%). Those materials were mixed by ball-milling in ethanol for 6 h using zirconia balls. The mixed powders were dried at 120 °C and calcined at 780 °C for 2 h. After calcination, the powders were pressed into disks with a diameter of 15 mm under 100 MPa using the solution of polyvinyl alcohol as binder. Through binder burn-out 500 °C, the samples were sintered at 1000 °C for 4 h. For the electrodes, the sintered samples were printed on both sides with silver at 850 °C. Samples for piezoelectric measurements were poled at 350 °C in air by applying a DC electric field of 1 kV/mm for 15–20 min. The electrical properties of all ceramics were measured more than 24 h later.

Phase structure of the ceramics was measured by X-ray diffraction (XRD) (D/max-2200, Rigaku, Japan, Cu K α) at room temperature. Surface microstructures of the ceramics were observed using a scanning electron microscopy (SEM) (model Quanta200, FEI Co.). Density is measured by the Archimedes method with distilled water. Dielectric properties were obtained using an Agilent E4980A by measuring the capacitance (C), dielectric constant ϵ_r and dielectric loss $\tan \delta$ at 1 kHz, 10 kHz, and 100 kHz as a function of temperature. The piezoelectric constant d_{33} was recorded at room temperature from 1 day aged samples using a quasi static piezoelectric d_{33} meter (ZJ-3d, China). The planar electromechanical coupling coefficient (K_p) is determined at room temperature by the resonance and anti-resonance techniques using an impedance analyzer (4294A).

The parameters f_r and K_p were measured in different temperatures. The HP 4294A were carried out at intervals of 20 °C from –20 °C to +120 °C with the temperature rising and fall. The equations used for $\Delta f_r/f_{r25\text{ °C}}$ and $\Delta K_p/K_{p25\text{ °C}}$ calculations are as follows:

$$\frac{\Delta f_r}{f_{r25\text{ °C}}} = \frac{f_r - f_r(25\text{ °C})}{f_r(25\text{ °C})} \times 100\% \quad (1)$$

$$\frac{\Delta k_p}{k_{p25\text{ °C}}} = \frac{k_p - k_p(25\text{ °C})}{k_p(25\text{ °C})} \times 100\% \quad (2)$$

The piezoelectric ceramics bimorph were fabricated by using the tape-casting technique, and then were sintered at 1000 °C for 4 h in a sealed alumina crucible. The sintered samples were polished after an ultrasonic cleaning in an ethanol bath. Silver-paste was coated to piezoelectric ceramics bimorph with dimensions L (44.95 ± 0.15) mm \times W (7.15 ± 0.15) mm \times T (0.245 ± 0.003) mm on both sides by the screen printing method, then subsequently fired at 850 °C for 30 min. The piezoelectric ceramics bimorph were poled at 350 °C for 30 min under a dc electric field of 1 kV/mm in air. The displacements of the piezoelectric ceramics bimorph were

measured by DGS-6C type Micro-displacement Test Instrument. In addition, the ambient temperature during the experiment was 21 °C.

3. Results and discussion

3.1. Phase structure

Fig. 1 shows the XRD patterns and c/a ratio of the ceramics sintered at 1000 °C with different Zr/Ti ratios. The tetragonal phase is obtained in all ceramics. As shown in Fig. 1, the c/a ratio decreases with the increasing of the Zr/Ti ratio, that is to say that tetragonality strongly decreases with the increasing of the Zr/Ti ratio. When the Zr/Ti ratio is approached to 1.041, the c/a ratio is close to 1 which indicates the points is in the MPB and lean to rhombohedral phase. The substitution of Zr^{4+} for Ti^{4+} will result in a small distortion on the octahedron because of the larger radius of Zr^{4+} than that of Ti^{4+} . Consequently, the substitution of ZrO_6 octahedrons for TiO_6 octahedrons will result in the $\text{Pb}(\text{Zr}_x\text{Ti}_{1-x})\text{O}_3\text{--Pb}(\text{Zn}_{1/3}\text{Nb}_{2/3})\text{O}_3\text{--Pb}(\text{Ni}_{1/3}\text{Nb}_{2/3})\text{O}_3$ cell enlargement.

3.2. Piezoelectric and dielectric properties

Fig. 2 shows d_{33} , K_p and Q_m of ceramics sintered at 1000 °C as functions of Zr/Ti ratio. Piezoelectric constant d_{33} and K_p increases with the increasing of Zr/Ti ratio. The maximum value of d_{33} (552 pC/N) is obtained at Zr/Ti ratio = 0.985. And then the values d_{33} decrease. The piezoelectric properties are degraded by the liquid phase in grain boundary because a very small scale formation of secondary phases at the grain boundary which inhibit the movement of domain walls in the process of polarization [11]. K_p and d_{33} show the same tendency. The maximum K_p value (0.77) is obtained at Zr/Ti = 0.985. Mechanical quality factor Q_m strongly drops with the increasing of the Zr/Ti ratio. According to the above results, the composition at Zr/Ti ratio = 0.985, which close to the MPB, shows the optimized values of d_{33} , K_p and Q_m , which are 552 pC/N, 0.77 and 70, respectively.

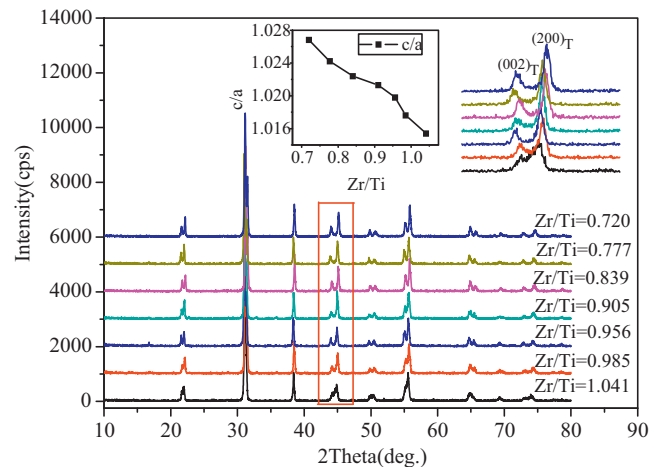


Fig. 1. XRD patterns and c/a ratio of ceramics sintered at 1000 °C with different Zr/Ti ratios, where Zr/Ti = 0.720, 0.777, 0.839, 0.905, 0.956, 0.985 and 1.041.

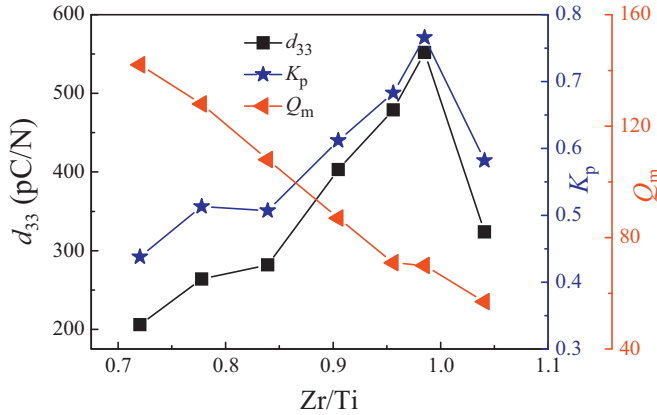


Fig. 2. d_{33} , K_p and Q_m of the ceramics sintered at 1000 °C as functions of Zr/Ti ratio.

Fig. 3 shows ϵ_r and $\tan \delta$ of the unpoled and poled ceramics sintered at 1000 °C as functions of the Zr/Ti ratio. It is observed that $\tan \delta$ of unpoled and poled ceramics has the same tendency with the increase of the Zr/Ti ratio. Dielectric loss $\tan \delta$ increases at first and it increases abruptly when the Zr/Ti ratio is above 0.985. The dielectric constant ϵ_r of the poled and unpoled ceramics shows the similar tendency. With the increase of the Zr/Ti ratio, ϵ_r increases at first, and then decrease. The maximum values of ϵ_r (2446 and 1628) of the poled and unpoled ceramics are attained at the Zr/Ti ratio = 0.985 and 0.956, respectively. As we know, factors that may affect ϵ_r of the ceramics with different Zr/Ti ratios include composition, micro-structural features (porosity, cracks, flaws, second phases).

The relative dielectric constant increment value $\Delta\epsilon_r$ is calculated as follows:

$$\Delta\epsilon_r = \frac{\epsilon_r(\text{poled}) - \epsilon_r(\text{unpoled})}{\epsilon_r(\text{unpoled})} \quad (3)$$

where $\epsilon_r(\text{poled})$ and $\epsilon_r(\text{unpoled})$ are the relative dielectric constants ϵ_r of poled and unpoled samples, respectively. As shown in Fig. 3, $\Delta\epsilon_r$ increases with the increasing of Zr/Ti ratio and attains the maximum value of 63% with the Zr/Ti ratio = 0.985, and then decreases. The variations of ϵ_r through poling are

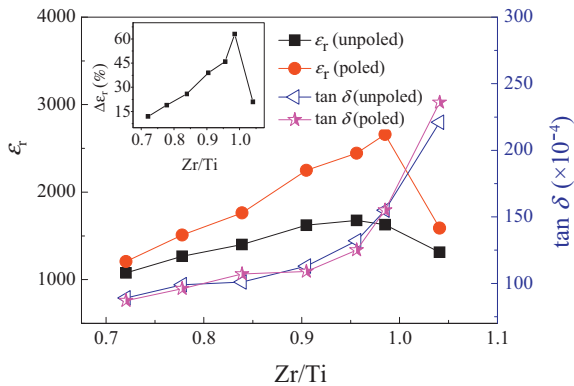


Fig. 3. ϵ_r and $\tan \delta$ of the unpoled and poled ceramics sintered at 1000 °C as functions of the Zr/Ti ratio.

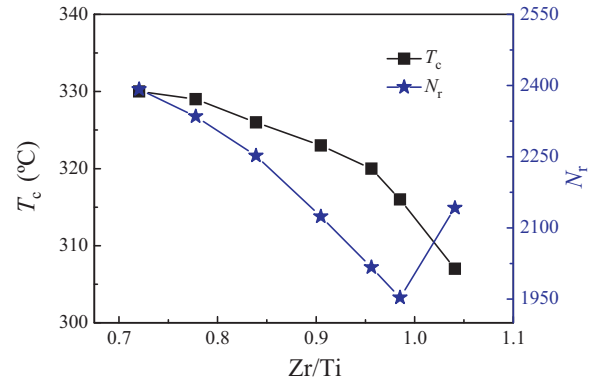


Fig. 4. N_r and T_c of ceramics sintered at 1000 °C as functions of Zr/Ti ratio.

explained as being due to the domain alignment. After the ceramics is polarized, the virtually complete 180° domain reorientation along the poling direction lead to the elimination of the clamping effect of 180° domains which induced the increase of ϵ_r . On the other hand, the anisotropy results in the decrease of ϵ_r . In a tetragonal phase, the removal of the clamping effect of 180° domains dominated the anisotropy with the result of a rise of ϵ_r after poling; and in a rhombohedral phase, the dielectric constant decrease after poling, and ϵ_r decrease is owing to the anisotropy dominating the removal of the clamping effect [12–14].

Fig. 4 shows frequent constant N_r and Curie temperature T_c of ceramics sintered at 1000 °C as functions of Zr/Ti ratio. With the increasing of the Zr/Ti ratio, N_r decreases and attains the lower value at the Zr/Ti ratio = 0.985, and then increases. T_c decreases with the increase of Zr/Ti ratio. The ceramics with the lattice constant (as shown in Fig. 1), the c/a ratio decreases with the increasing of the Zr/Ti ratio. It means that the decrease of tetragonality might contribute to the decrease of the Curie temperature [15]. On the other hand, because of the PbTiO_3 has a high Curie temperature ($T_c = 490$ °C), while PbZrO_3 has a comparatively low Curie temperature ($T_c = 230$ °C). The PbZrO_3 ingredient increases with the increasing of the Zr/Ti ratio, so the Curie temperature T_c decreases with the increasing of Zr/Ti ratio. To avoid the transition from ferroelectric to paraelectric state occurring in the operating temperature range for bimorph, the higher Curie temperature is needed for piezoelectric materials. The Curie temperature of the ceramics is 316 °C when the Zr/Ti ratio is 0.985, which is suitable to be used in piezoelectric ceramics bimorphs.

3.3. Temperature stability

Fig. 5 shows $\Delta f_r/f_{r25\text{ }^\circ\text{C}}$ of PZT–PZN–PNN ceramics as a function of Zr/Ti ratio. With the increasing of the Zr/Ti ratio, the temperature coefficient of resonant frequency $\Delta f_r/f_{r25\text{ }^\circ\text{C}}$ increases at 40, 80 and 120 °C and get the higher value at the Zr/Ti ratio (0.956), and then decreases. When the testing temperature is –20 °C, $\Delta f_r/f_{r25\text{ }^\circ\text{C}}$ of the ceramics has the inverse tendency with the temperature of 40, 80 and 120 °C. $\Delta f_r/f_{r25\text{ }^\circ\text{C}}$ of the ceramics with Zr/Ti ratio = 0.985 is close to zero approximately in all the temperature range. It can be seen

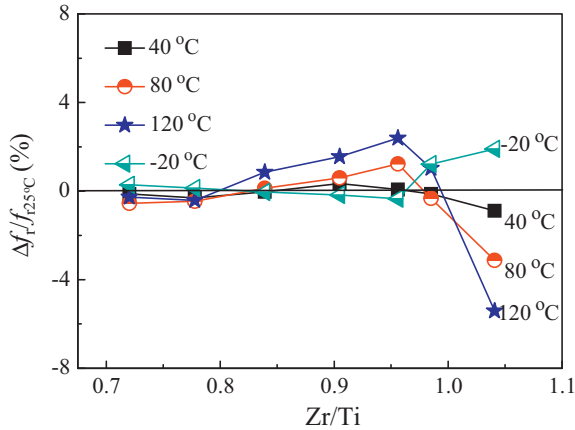


Fig. 5. $\Delta f_r/f_{r25^\circ\text{C}}$ of PZT–PZN–PNN ceramics as a function of Zr/Ti ratio.

that $\Delta f_r/f_{r25^\circ\text{C}}$ shifts from plus (+) to minus (–) value with the increasing of Zr/Ti ratio and obtains a minimum value at Zr/Ti = 0.985. The variation of $\Delta f_r/f_{r25^\circ\text{C}}$ is believed to be mainly due to the change of the elastic compliance coefficient [16]. The increases of the elastic compliance coefficient result in the decreases of resonant frequency. As been proposed by Zhang et al. [13], the temperature stability is related to the domain structure and domain wall motions, and the whole crystal grain motions induced by non-180° domain wall motions generate elastic deformation and then create internal stress field in ceramics, which finally reduce elastic compliance coefficient.

Fig. 6 shows $\Delta K_p/K_{p25^\circ\text{C}}$ of the PZT–PZN–PNN ceramics as a function of Zr/Ti ratio. The temperature coefficient of electromechanical coupling factor $\Delta K_p/K_{p25^\circ\text{C}}$ has the inverse tendency with the $\Delta f_r/f_{r25^\circ\text{C}}$ of the ceramics and get the lower value in Zr/Ti = 0.985. It can be explained by the relationship between the electromechanical coupling factor and the resonant frequency. The electromechanical coupling factor k_p of the ceramics is calculated as follows:

$$k_p = \sqrt{\frac{2.51 \times (f_a - f_r)}{f_r}} \quad (4)$$

where the f_r and f_a are resonant and anti-resonant frequencies. It can be seen that $\Delta K_p/K_{p25^\circ\text{C}}$ of the ceramics is mainly

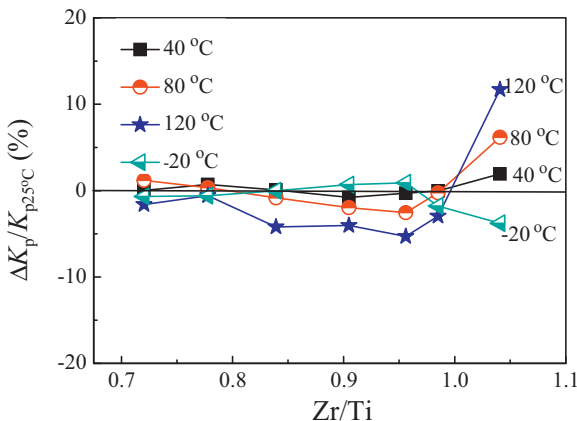


Fig. 6. $\Delta K_p/K_{p25^\circ\text{C}}$ of PZT–PZN–PNN ceramics as a function of Zr/Ti ratio.

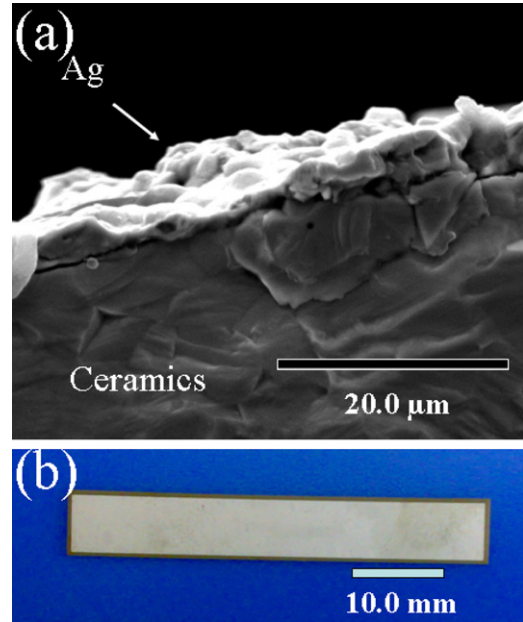


Fig. 7. The fracture surface SEM micrographs and sample picture of the piezoelectric ceramics bimorph sintered at 1000 °C.

determined by the temperature dependence of f_r/f_a . As shown in Fig. 6, $\Delta K_p/K_{p25^\circ\text{C}}$ of the ceramics with Zr/Ti ratio = 0.985 approaches to zero in all the temperature ranges. This is in accordance with the $\Delta f_r/f_{r25^\circ\text{C}}$ of the ceramics in Fig. 5. Taking into consideration the temperature coefficient and the electrical properties of the ceramics, the composition with Zr/Ti ratio (0.985) can be selected as the optimized composition used in bimorphs.

3.4. Fabrication and characteristics of piezoelectric ceramics bimorph

According to the above results, the piezoelectric ceramic bimorphs with Zr/Ti ratio (0.985) have been prepared using the piezoelectric ceramic membrane obtained by the tape-casting method. The fracture surface SEM micrographs and sample picture of the piezoelectric ceramics bimorph sintered at

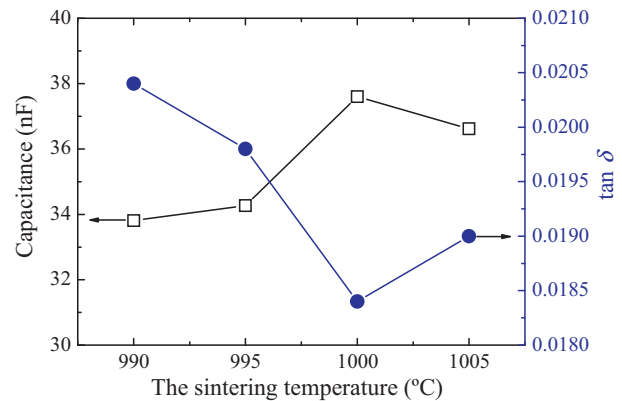


Fig. 8. Capacitance and tan δ of the poled piezoelectric ceramics bimorph sintered at 1000 °C as functions of the sintering temperature.

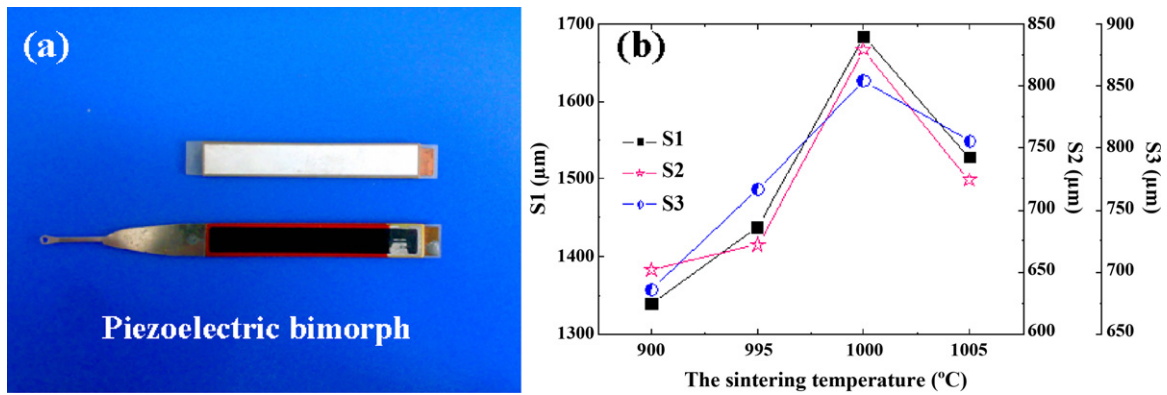


Fig. 9. (a) The photograph of configuration of piezoelectric ceramics bimorph. (b) The displacement curves of the piezoelectric ceramics bimorph as a function of the sintering temperature.

1000 °C are shown in Fig. 7. It can be seen from Fig. 7(a) that the membrane has low porosity, high density, clear and continued Ag alloy layer. The piezoelectric ceramics bimorph make up the needle selecting mechanism of the electronic jacquard. The properties of the piezoelectric ceramics bimorph are not only determined by the piezoelectric and dielectric properties of the ceramics, but also strongly affected by the length, width and the heights of the ceramics, and the thickness of the middle steel flake. The piezoelectric ceramic bimorphs with dimensions (44.95 ± 0.15) mm length \times (7.15 ± 0.15) mm width \times (0.245 ± 0.003) mm thickness are poled in Fig. 7(b). Fig. 8 shows capacitance (nF) and $\tan \delta$ of PZT–PZN–PNN ceramics bimorph as functions of the sintering temperature. Capacitance increases with increasing of the sintering temperature. The maximum capacitance value (37.6 nF) is obtained at 1000 °C because of the densification and the uniform microstructure of the ceramics with fewer pores, and then capacitance decreases. The dielectric loss and ϵ_r show the reverse tendency of variation with increasing sintering temperature. The dielectric loss decreases and the minimum $\tan \delta$ value (0.0184) are obtained at 1000 °C. When the sintering temperature is beyond 1000 °C, the dielectric constant decreases while $\tan \delta$ increases. Fig. 9(a) shows the photograph configuration of the piezoelectric ceramics bimorph used in the needle selecting mechanisms. Fig. 9(b) shows the displacement of the piezoelectric ceramics bimorph at the working voltage of 180 V as a function of the sintering temperature. The plus (+) displacement (S2) increases with the increasing of the sintering temperature. The maximum S2 value (+804 μm) is obtained at 1000 °C, and then S2 decreases. The S3 curve indicates a negative, depressed direction that is on the opposite side of the typical displacement curve of bulk PZT–PZN–PNN based piezoelectric ceramics bimorph. The absolute value (S3) of the minus (–) displacement decreases with the increasing of the sintering temperature. The maximum S3 value (879 μm) is obtained at 1000 °C, and then S3 increases. This displacement property appears to indicate a deflection motion of PZT–PZN–PNN based piezoelectric ceramics bimorph. The longitudinal displacement changes from the positive to the negative direction. The value of maximum displacement S1

(S2 + S3) is 1683 μm at the applied voltage of 180 V. These results suggest that the deflection motion is dominant for the negative displacement and the longitudinal strain caused by the transversal piezoelectric effect is dominant for the positive displacement. The results show that the piezoelectric ceramics bimorph have good electrical properties and larger displacement which can satisfy the requirements of practical needle selecting mechanisms applications.

4. Conclusions

The effects on different Zr/Ti ratios for PZT–PZN–PNN ceramics have been investigated. The piezoelectric ceramics bimorph are fabricated successfully for PZT–PZN–PNN ceramics at Zr/Ti ratio = 0.985. And the characteristics of the bimorph are also investigated. The following conclusions have been obtained:

- (1) $\text{Pb}(\text{Zr}_x\text{Ti}_{1-x})\text{O}_3\text{--Pb}(\text{Zn}_{1/3}\text{Nb}_{2/3})\text{O}_3\text{--Pb}(\text{Ni}_{1/3}\text{Nb}_{2/3})\text{O}_3$ ceramics with Zr/Ti ratio = 0.985 sintered at 1000 °C exhibit the optimal electrical properties, which are listed as follows: $d_{33} = 552$ pC/N, $K_p = 0.77$, $Q_m = 70$, $\tan \delta = 0.0150$ and $\epsilon_r = 2659$. With the increasing of the Zr/Ti ratio, the frequency constant N_r decreases and the minimum value obtains at the Zr/Ti ratio = 0.985, and then increases. When the Zr/Ti ratio is 0.985, the curves of $\Delta f_r/f_{r25^\circ\text{C}}$ and $\Delta K_p/K_{p25^\circ\text{C}}$ show the inverse tendency and fluctuate around the zero line, which indicate that the favorable temperature stability are obtained.
- (2) The piezoelectric ceramics bimorph with dimensions (44.95 ± 0.15) mm length \times (7.15 ± 0.15) mm width \times (0.245 ± 0.003) mm thickness are fabricated successfully using PZT–PZN–PNN ceramics with Zr/Ti = 0.985 by the tape-casting technology. The piezoelectric ceramics bimorph sintered at 1000 °C exhibited larger displacement of 1683 μm at the working voltage of 180 V.

This piezoelectric ceramics bimorph has a high electrical properties, large displacement and high response, which is very suitable for the practical needle selecting mechanisms applications.

Acknowledgements

This work was supported by National Science Foundation of China (NSFC) (Grant No. 51172136 and No. 51107077), Natural Science Research Program of Shaanxi Province (Grant No. 2009JZ003) and the Fundamental Research Funds for the Central Universities (Program No. 2010ZYGX011).

References

- [1] A. Shafiei, T. Nickchi, C. Oprea, A. Alfantazi, T. Troczynski, Investigation of hydrogen effects on the properties of $\text{Pb}(\text{Zr,Ti})\text{O}_3$ in tetragonal phase using water electrolysis technique, *Appl. Phys. Lett.* 99 (2011) 212903.
- [2] Y.J. Cha, I.T. Seo, I.Y. Kang, S.B. Shin, J.H. Choi, et al., Effect of the structural properties on the energy density of $\text{Pb}(\text{Zr}_{0.47}\text{Ti}_{0.53})\text{O}_3$ – $\text{Pb}[(\text{Ni}_{0.6}\text{Zn}_{0.4})_{1/3}\text{Nb}_{2/3}]\text{O}_3$ ceramics, *J. Appl. Phys.* 110 (2011) 084111.
- [3] X.L. Chao, Z.P. Yang, L.R. Xiong, Z. Li, Effect of addition of $\text{Ba}(\text{W}_{0.5}\text{Cu}_{0.5})\text{O}_3$ in $\text{Pb}(\text{Mg}_{1/3}\text{Nb}_{2/3})\text{O}_3$ – $\text{Pb}(\text{Zn}_{1/3}\text{Nb}_{2/3})\text{O}_3$ – $\text{Pb}(\text{Zr}_{0.52}\text{Ti}_{0.48})\text{O}_3$ ceramics on the sintering temperature, electrical properties and phase transition, *J. Alloys Compd.* 509 (2011) 512–517.
- [4] G. Deng, A. Ding, X. Zheng, X. Zeng, Q. Yin, Property improvement of $0.3\text{Pb}(\text{Zn}_{1/3}\text{Nb}_{2/3})\text{O}_3$ – $0.7\text{Pb}_{0.96}\text{La}_{0.04}(\text{Zr}_x\text{Ti}_{1-x})0.99\text{O}_3$ ceramics by hot-pressing, *J. Eur. Ceram. Soc.* 26 (2006) 2349–2355.
- [5] J.Y. Ha, J.W. Choi, C.Y. Kang, D.J. Choi, H.J. Kim, S.J. Yoon, Effects of ZnO on piezoelectric properties of 0.01PMW – 0.41PNN – 0.35PT – 0.23PZ ceramics, *Mater. Chem. Phys.* 90 (2005) 396–400.
- [6] Z.P. Yang, X.L. Chao, R. Zhang, Y.F. Chang, Y.Q. Chen, Fabrication and electrical characteristics of piezoelectric PMN–PZN–PZT ceramic transformers, *Mater. Sci. Eng. B* 138 (2007) 277–283.
- [7] S.S. Zhao, H. Wu, Q.C. Sun, Study on PSN–PZN–PZT quaternary piezoelectric ceramics near the morphotropic phase boundary, *Mater. Sci. Eng. B* 123 (2005) 203–210.
- [8] G.M. Lee, B.H. Kim, Effects of thermal aging on temperature stability of $\text{Pb}(\text{Zr}_x\text{Ti}_{1-x})\text{O}_3 + x(\text{wt.}\%)\text{Cr}_2\text{O}_3$ ceramics, *Mater. Chem. Phys.* 91 (2005) 233–236.
- [9] M. Alguero, A. Moure, L. Pardo, J. Holc, M. Kosec, Processing by mechanosynthesis and properties of piezoelectric $\text{Pb}(\text{Mg}_{1/3}\text{Nb}_{2/3})\text{O}_3$ – PbTiO_3 with different compositions, *Acta Mater.* 54 (2006) 501–511.
- [10] X.L. Chao, D.F. Ma, R. Gu, Z.P. Yang, Effects of CuO addition on the electrical responses of the low-temperature sintered $\text{Pb}(\text{Zr}_{0.52}\text{Ti}_{0.48})\text{O}_3$ – $\text{Pb}(\text{Mg}_{1/3}\text{Nb}_{2/3})\text{O}_3$ – $\text{Pb}(\text{Zn}_{1/3}\text{Nb}_{2/3})\text{O}_3$ ceramics, *J. Alloys Compd.* 491 (2010) 698–702.
- [11] L. Sun, C.D. Sun, Q.C. Feng, H. Zhou, Study on $\text{Pb}(\text{Zr,Ti})\text{O}_3$ – $\text{Pb}(\text{Zn}_{1/3}\text{Nb}_{2/3})\text{O}_3$ – $\text{Pb}(\text{Sn}_{1/3}\text{Nb}_{2/3})\text{O}_3$ – $\text{Pb}(\text{Mn}_{1/3}\text{Sb}_{2/3})\text{O}_3$ quinary system piezoelectric ceramics, *Mater. Sci. Eng. B* 122 (2005) 61–66.
- [12] Y.D. Hou, P.X. Lu, M.K. Zhu, X.M. Song, J.L. Tang, B. Wang, H. Yan, Effect of Cr_2O_3 addition on the structure and electric properties of $\text{Pb}(\text{Zn}_{1/3}\text{Nb}_{2/3})_{0.20}(\text{Zr}_{0.50}\text{Ti}_{0.50})_{0.80}\text{O}_3$ ceramics, *Mater. Sci. Eng. B* 116 (1) (2005) 104–108.
- [13] Q.M. Zhang, H. Wang, N. Kim, Direct evaluation of domain-wall and intrinsic contributions to the dielectric and piezoelectric response and their temperature dependence on lead zirconate–titanate ceramics, *J. Appl. Phys.* 75 (1994) 454–459.
- [14] G. Liu, W.H. Jiang, J.Q. Zhu, W.W. Cao, Electromechanical properties and anisotropy of single- and multi-domain $0.72\text{Pb}(\text{Mg}_{1/3}\text{Nb}_{2/3})\text{O}_3$ – 0.28PbTiO_3 single crystals, *Appl. Phys. Lett.* 99 (2011) 162901.
- [15] H.L. Du, Z.B. Pei, W.C. Zhou, F. Luo, S.B. Qu, Effect of addition of MnO_2 on piezoelectric properties of PNW–PMS–PZT ceramics, *Mater. Sci. Eng. A* 421 (2006) 286–289.
- [16] C. Cheon, J.S. Park, Temperature stability of the resonant frequency in Cr_2O_3 doped $\text{Pb}(\text{Zr,Ti})\text{O}_3$ ceramics, *J. Mater. Sci. Lett.* 16 (1997) 2043–2046.